3,5,2,3
3,4,3,2

~~CONFIDENTIAL~~ UNCLASSIFIED
~~SECRET~~

Copy
RM E56K28a

P1

RESEARCH MEMORANDUM

COMBUSTOR PERFORMANCE OF A 16-INCH RAM JET USING GASEOUS HYDROGEN AS FUEL AT MACH NUMBER 3.0

By Joseph F. Wasserbauer and Fred A. Wilcox

Lewis Flight Propulsion Laboratory
Cleveland, Ohio

NATIONAL ADVISORY COMMITTEE
FOR AERONAUTICS

WASHINGTON

January 18, 1957

NACA RM E56K28a

NATIONAL ADVISORY COMMITTEE FOR AERONAUTICS

RESEARCH MEMORANDUM

COMBUSTOR PERFORMANCE OF A 16-INCH RAM JET USING GASEOUS HYDROGEN AS FUEL AT MACH NUMBER 3.0

By Joseph F. Wasserbauer and Fred A. Wilcox

SUMMARY

An investigation was conducted in the NACA Lewis 10- by 10-foot supersonic wind tunnel to evaluate the performance of three burner configurations in a 16-inch ram jet with gaseous hydrogen as fuel. Data were obtained over a fuel-air-ratio range from 0.0030 to 0.0260 (stoichiometric = 0.0292) at a free-stream Mach number of 3.0 and 0° angle of attack. The exit nozzle-throat area ratios employed were 0.60 and 0.75.

Results of this investigation showed that a flameholding shroud fitted to an injector-burner greatly improved its performance. This flameholding shroud-injector combination gave high combustion efficiencies over a wide fuel-air-ratio range, reaching 93 percent near critical inlet operation, and operated very satisfactorily under inlet pulsing. The results also indicated that combustor tailpipe length, including the converging nozzle, could be shortened from 3 to 2 feet with only a 1-percentage-point drop in combustion efficiency at critical inlet conditions.

INTRODUCTION

Analytical evaluations of hydrogen (refs. 1 and 2) show that its physical properties make it a very desirable ram-jet fuel for high-altitude flight. A high-altitude ram jet requires a fuel that will burn with high efficiency at low combustor-inlet pressure in a short lightweight combustor. The wide flammability limits of hydrogen and high laminar flame speed (7.6 times that of JP-4) indicate that it should fulfill these requirements. Also, the high heating value of hydrogen makes it desirable from range considerations.

Ram-jet-combustor investigations using hydrogen as fuel have been conducted in direct-connect facilities only, and very satisfactory results have been obtained (refs. 3 and 4). However, combustor performance behind a supersonic inlet has not yet been demonstrated.

An investigation was therefore undertaken in the NACA Lewis 10- by 10-foot supersonic wind tunnel with a 16-inch ram-jet engine using gaseous hydrogen as fuel. The engine was equipped with a single-oblique-shock external-compression inlet, and its performance was investigated at a free-stream Mach number of 3.0 and at zero angle of attack. The specific objectives of the investigation were to evaluate the effect on combustion efficiency of (1) combustor configuration, (2) combustor-inlet Mach number (obtained by using different exit nozzle-throat areas), and (3) tailpipe length.

This report presents the internal engine and combustor behavior observed with three different combustor designs, two exit nozzles, and two tailpipe lengths. In addition, the effect of subcritical and pulsing inlet operation on combustor performance is discussed.

SYMBOLS

f	fuel-air ratio
l	length from burner to nozzle exit
M	Mach number
P	total pressure
$\frac{P_{max} - P_{min}}{P_{av}}$	flow-distortion parameter
p	static pressure
$\Delta p/p$	static-pressure amplitude, $(p_{max} - p_{min})/p_{av}$
T	total temperature
x	distance from burner
x/l	ratio of distance from burner to over-all combustor length
η_B	combustion efficiency
τ	total-temperature ratio, T_6/T_3
φ	equivalence ratio, ratio of f to stoichiometric f

Subscripts:

av	average
max	maximum
min	minimum
0	free-stream conditions
3	airflow measuring station (model station 65)
6	nozzle-throat or -exit station

APPARATUS AND PROCEDURE

A schematic diagram of the 16-inch-diameter ram-jet engine with which this study was made is shown in figure 1. The tests were conducted in the Lewis 10- by 10-foot supersonic wind tunnel, and the engine was supported by a fixed strut. The inlet for this model was adapted to an existing ram jet designed for operation with a hydrocarbon fuel at a Mach number of 2.0 and does not necessarily represent the optimum. The supersonic diffuser was designed so that the oblique shock generated by the 30°-half-angle cone intersected the cowl lip at a free-stream Mach number of 3.0. The centerbody was extended to position the burner downstream of the support strut and to minimize overheating of the engine support structure.

Inlet pressure recovery and subcritical mass flows were obtained from a static- and total-pressure survey at model station 65 (fig. 1). For critical and supercritical inlet operation, the stream-tube capture-area mass flow was used. A rake mass-flow calibration factor was obtained by comparing the computed mass flow with the capture-area stream-tube mass flow at critical inlet conditions. This calibration factor was then applied to the subcritical data. Because of the inlet pulsing resulting at nearly all subcritical conditions, the mass-flow measurement is less accurate; and, therefore, all data points in the figures are flagged in this operating region.

Exit total pressure at the throat of the choked nozzle was obtained from a water-cooled total-pressure tail rake as shown in figure 1. Exit total temperature was then calculated from the continuity relation. Combustion efficiency was calculated from the enthalpy rise of the gas divided by the available heat content of the fuel. Values used for enthalpy, ratio of specific heats, and gas constant were calculated from reference 5.

Of the burners investigated in this engine (fig. 2), burner 1 was of the same design as reported in reference 3 (configuration B) and burner 2 was based on the injector-burner designs of reference 4. Details of these two burner configurations are shown in figures 2(a) and (b). Burner 3 (fig. 2(c)) was obtained by adding a shroud to each injector bar of burner 1, to improve the lean fuel-air-ratio performance. The shroud was designed to maintain the local fuel-air ratio at the injection points near the stoichiometric value at an over-all burner fuel-air ratio of 0.0120. This value corresponds to an equivalence ratio φ of 0.4. The tabs at the downstream end of each shroud plate were deflected to act as turbulence generators. A photograph of burner 3 is shown in figure 2(d). The relative position of the burners and the tailpipe lengths used are indicated in figure 1.

Simple convergent nozzles, choked for all operating conditions, were used. Two contraction ratios, 0.60 and 0.75, were investigated. The combustor length, measured from the point of fuel injection to the exit nozzle throat, was nominally maintained at 3 feet. Burner 2 was also evaluated with a 2-foot combustor length.

The hydrogen was stored as a gas in cylinder tanks at a pressure of 2400 pounds per square inch gage. Fuel was taken directly from the storage cylinders through a pressure-reducing valve, metering orifice, and throttling valve to the engine.

Frequency and amplitude of the internal pressure fluctuations were measured with a dynamic pickup and recorded with a commercial oscillograph. The galvanometer elements in the oscillograph had a natural frequency of 200 cycles per second. The dynamic pickup was located at the airflow measuring station (station 65).

The tests were made at a tunnel Mach number of 3.0 and at a simulated pressure altitude of 71,000 feet. The tunnel total temperature was $664^{\circ} \pm 8^{\circ}$ R.

RESULTS AND DISCUSSION

General combustor performance data of the three burner configurations investigated are presented in figure 3. Included in the figure are the variation with fuel-air ratio of combustion efficiency η_B, combustor total-temperature ratio τ, and the combustion-chamber-inlet Mach number M_3. Burners 1 and 2 were tested with exit nozzles of both 0.60 and 0.75 contraction ratio. Burner 3 was tested only with the 0.75-contraction-ratio nozzle. Data points for subcritical inlet operating conditions are flagged.

The combustor performance of burner 1 is shown in figure 3(a). With the 0.60 exit nozzle, this burner would not operate in the subcritical range ($M_3 < 0.175$). As the inlet went into pulsing, blowout occurred. Apparently, the fuel-air ratio was so lean (0.007) and the change in η_B with fuel-air ratio so rapid that the severe condition of inlet pulsing prevented continued combustion. Although lean blowout was not determined, reducing the fuel-air ratio below 0.007 caused a sharp drop in combustion efficiency. This decrease can be attributed to (1) increased flow distortions, resulting from supercritical inlet operation, (2) poor fuel penetration at low fuel flow, and (3) increased combustion-chamber-inlet Mach number. Reference 3 reports testing this burner with a 0.50 nozzle in a connected-pipe facility. A wider range of fuel-air ratio was obtained; however, the burner-inlet velocities were lower, and neither flow distortions nor inlet pulsing was present. A curve from the data of reference 3 is included in figure 3(a).

The 0.75 nozzle operated over a wider range of fuel-air ratio. Combustion during subcritical operation with inlet pulsing was possible with this nozzle because of the higher fuel-air ratios existing at critical and subcritical inlet conditions. Comparison of burner behavior with the two different nozzle sizes shows that supercritical operation with the 0.75 nozzle occurs at a lower rate of combustion-efficiency change with fuel-air ratio. This probably happens because a higher fuel-air-ratio level is required for operation with the larger nozzle. It is interesting to note that essentially the same combustion efficiency resulted at a given combustion-chamber-inlet Mach number irrespective of nozzle size and fuel-air ratio.

Burner 2 (fig. 3(b)) operated at much higher combustion efficiencies than burner 1 with the 0.60 nozzle. Combustion was maintained during inlet pulsing and reached 90 percent at critical, compared with 83 percent for burner 1. This improved efficiency is attributed to the increased number of injection points, resulting in a more even distribution of the fuel. Essentially the same efficiency level was obtained with this burner operating with a 0.60 nozzle as was reported with a 0.50 nozzle during testing in a connected-pipe facility (ref. 4). A curve from the data of reference 4 is included in figure 3(b) for comparison.

With the 0.75 nozzle and burner 2, combustion efficiencies at or near critical were about 80 percent and lower than those of burner 1. However, for supercritical operation better efficiencies were observed with burner 2. This improvement is also attributed to the increased number of injection points.

Because of the low penetration of hydrogen into a high-velocity airstream, the philosophy adopted in the design of burner configurations 1 and 2 was to inject fuel at a large number of points. During development of burner 1 (ref. 3) a V-gutter was used as a flameholder in addition to the injector. Little improvement was achieved with this arrangement over the basic injector configuration. It was therefore concluded that flameholders inserted to perform the sole function of turbulence generation were ineffective in raising burner efficiency. However, data presented herein show a rapid decrease in combustion efficiency at the low fuel-air ratio and a generally lower than expected level of combustion efficiency. This indicates that gains in burner performance were needed, even with a super-fuel such as hydrogen.

In an attempt to raise the efficiency at lean fuel-air ratios, techniques proved successful with ordinary hydrocarbon fuels were applied to the design of a hydrogen burner configuration. The injector and ignitor features of burner 1 were retained, but a shroud was added to each injector bar (figs. 2(c) and (d)). The shroud was designed to retain a locally stoichiometric mixture at an over-all equivalence ratio of 0.4 and had, in addition, bent tabs that served a flameholding function at the trailing edge. This configuration is designated burner 3.

With a 0.75 nozzle, burner 3 exhibited the best performance obtained during these tests (fig. 3(c)). A constant combustion efficiency of 93 percent was observed from critical inlet operation at a fuel-air ratio of 0.0135 to a supercritical condition at a fuel-air ratio of 0.0095. Combustion efficiencies of 80 percent or better were maintained to fuel-air ratios as lean as 0.0067. Further decreases in fuel-air ratio resulted in a rapid decrease in combustion efficiency and ultimate blowout at a fuel-air ratio of about 0.0038, the leanest fuel-air ratio attained with any burner in this investigation.

As a point of interest, the combustion-efficiency curve of the flameholder configuration is included in figure 3(c) from data given in reference 3. No direct comparison should be made between the flameholder configuration of reference 3 and burner 3 reported herein, since the performance of the former is with a 0.50 nozzle and the latter with a 0.75 nozzle. However, it may be concluded that, of the two, burner 3 has a leaner blowout point and operates at essentially the same level of efficiency as the flameholder configuration of reference 3 but has considerably greater burner-inlet velocities and greater airflow distortions.

The combustion efficiencies of the three burners investigated with a 0.75 exit nozzle and a 3-foot pipe length are compared in figure 4. The superior performance of burner 3 over burners 1 and 2 is evident. The aims of the flameholding-shroud design to promote mixing and to control the mixture distribution were achieved. Considerable gains in the level of combustion efficiency and extension of the lean limit were

obtained. It should be noted that burner 2 has essentially the same curve shape as burner 3, but at a displaced fuel-air ratio and with a reduced combustion-efficiency level.

The total-pressure drop across the combustion chamber during burning with the 3-foot tailpipe length and the 0.75 nozzle is presented for the three burners investigated in figure 5. The improved performance of burner 3 was expected to be accompanied by an increased total-pressure drop across the combustion chamber. However, the data of figure 5 show that the flameholding shroud had only $1\frac{1}{2}$ percentage points more pressure drop than the burner 1 fuel-injector configuration, but $3\frac{1}{2}$ percentage points less than the pressure drop across burner 2.

The effect of combustor length on combustion efficiency was investigated with burner 2 and a 0.75 nozzle. Figure 6(a) shows the static-pressure distribution along the three-foot tailpipe for several operating conditions. Apparently, the heat release occurred primarily in the first 0.7 of the total pipe length, for beyond this point the static pressure appears to level off. Therefore, it was concluded that the length could be shortened without reducing combustion efficiency. The tailpipe was then shortened to a total length of only 2 feet; the static-pressure distribution for this latter configuration is given in figure 6(b). At critical inlet operation, the combustion efficiency was decreased only 1 percentage point because of shortening the tailpipe (fig. 7). Operation at leaner fuel flows resulted in a somewhat greater loss in efficiency.

The variation of diffuser total-pressure recovery with combustion-chamber-inlet Mach number obtained during burner operation is presented in figure 8. As expected, no effect of burner design on diffuser performance was noted. Peak pressure recovery of 0.525 at a critical Mach number of 0.175 was obtained with all three burners. Little or no subcritical stability with any of the three burners was observed.

Flow distortion at the airflow measuring station is presented in figure 9. The distortion level appears to be essentially the same with all three combustors. In the subcritical region, flow distortion is low, about 4 percent. However, as would be expected, the distortion level increased rapidly in the supercritical region of inlet operation. It should be noted that burner 3 operating with a measured inlet flow distortion of about 11 percent had a combustion efficiency of 90 percent.

Typical burner-inlet total-pressure profiles experienced behind the supersonic inlet are presented in figure 10. Generally, these profiles were not greatly influenced by burner design but rather by the inlet operating condition. Severest flow distortion, as indicated in figure 9 and emphasized in figure 10, occurred during supercritical inlet operation.

It is apparent that, because of the distortion in the total pressure and consequently in the velocity profiles at the burner inlet, the performance of a burner designed from connected-pipe tests having uniform inlet flow will, in general, be unfavorably affected when combined with a supersonic inlet.

The subcritical pulsing frequencies and amplitudes observed are presented in figure 11. With burner 2, a marked decrease in static-pressure amplitude and a shift in the initial pulse frequencies were observed when the tailpipe length was reduced from 3 to 2 feet. This result is in agreement with the effect of chamber length on buzz predicted in reference 6. In spite of its higher pressure drop and expected greater damping force, at the same combustion-chamber length the pulse amplitudes with burner 2 were significantly greater than those of burner 3. Burner 3 operated satisfactorily and with high efficiencies at static-pressure amplitudes of 35 percent. With the same burner length, no significant effect on pulse frequency was observed between burners 2 and 3. In general, it can be concluded that the burner configurations can be operated satisfactorily under severe inlet pulsing conditions.

SUMMARY OF RESULTS

The following results were obtained during the study in the NACA Lewis 10- by 10-foot supersonic wind tunnel of the internal performance of a 16-inch ram jet using gaseous hydrogen as a fuel at a Mach number of 3.0:

1. Addition of a flameholding shroud to an injector-burner greatly improved its performance. The combustion efficiencies were increased more than 10 percentage points over the range of stable inlet operation, and the lean blowout limit was extended.

2. Combustion efficiencies exceeding 90 percent at flow distortions of about 11 percent were obtained with the shrouded burner. In addition, burner operation during inlet pulsing at static-pressure amplitudes up to 35 percent was obtained.

3. For one of the burner configurations investigated, the tailpipe length was shortened from 3 to 2 feet with only a 1-percentage-point decrease in combustion efficiency at critical inlet operation.

Lewis Flight Propulsion Laboratory
National Advisory Committee for Aeronautics
Cleveland, Ohio, November 29, 1956

REFERENCES

1. Silverstein, Abe, and Hall, Eldon W.: Liquid Hydrogen as a Jet Fuel for High-Altitude Aircraft. NACA RM E55C28a, 1955.

2. Henneberry, Hugh M.: Effect of Fuel Density and Heating Value on Ram-Jet Airplane Range. NACA RM E51L21, 1952.

3. Dangle, E. E., and Kerslake, William R.: Experimental Evaluation of Gaseous Hydrogen Fuel in a 16-Inch-Diameter Ram-Jet Engine. NACA RM E55J18, 1955.

4. Krull, H. George, and Burley, Richard R.: Effect of Burner Design Variables on Performance of 16-Inch-Diameter Ram-Jet Combustor Using Gaseous Hydrogen Fuel. NACA RM E56J08, 1956.

5. Huff, Vearl N., Gordon, Sanford, and Morrell, Virginia E.: General Method and Thermodynamic Tables for Computation of Equilibrium Composition and Temperature of Chemical Reactions. NACA Rep. 1037, 1951. (Supersedes NACA TN's 2113 and 2161.)

6. Sterbentz, William H., and Davids, Joseph: Amplitude of Supersonic Diffuser Flow Pulsations. NACA TN 3572, 1955. (Supersedes NACA RM E52I24.)

[redacted]

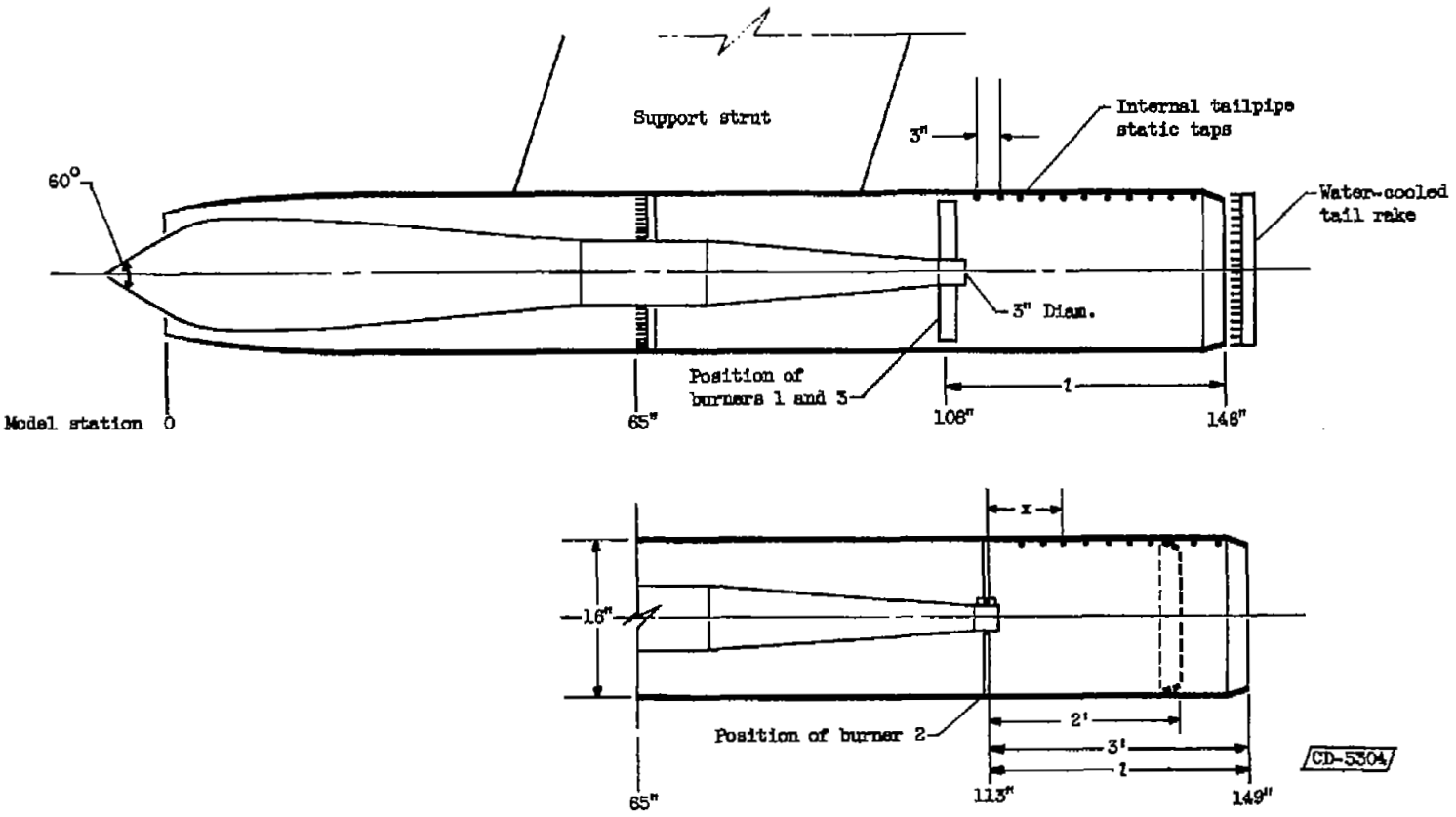

Figure 1. - 16-Inch-diameter ram jet in 10- by 10-foot tunnel.

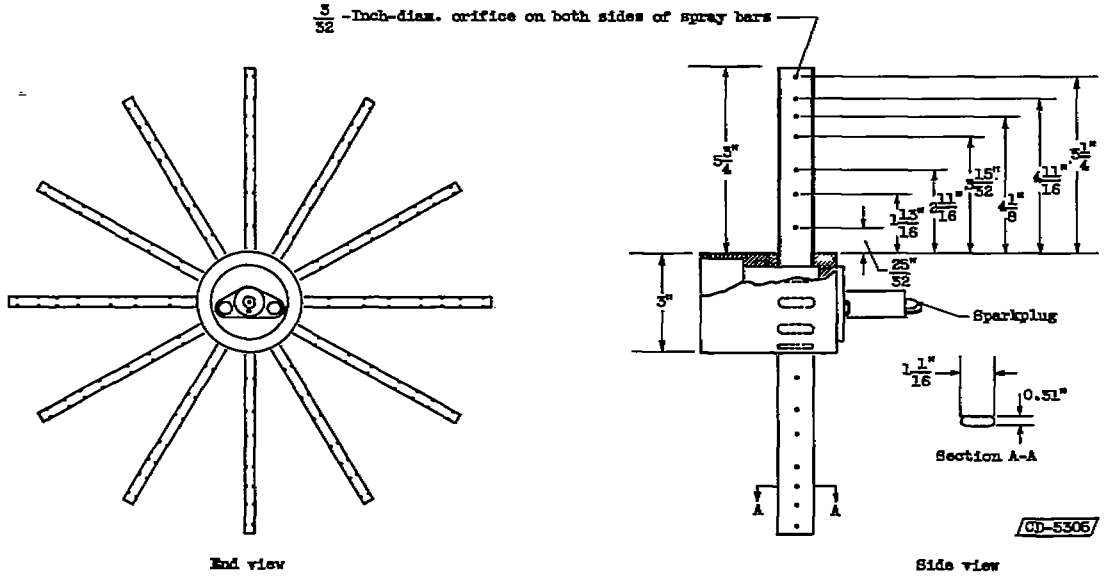

(a) Burner 1.

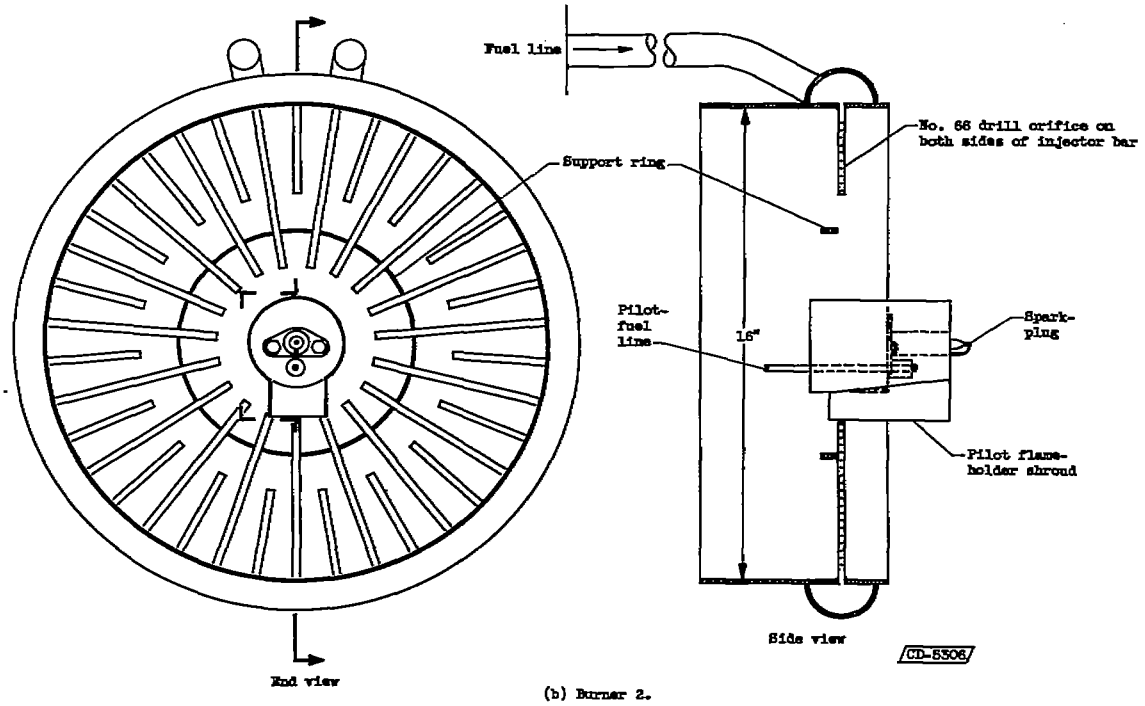

(b) Burner 2.

Figure 2. - Burners investigated.

[redacted]

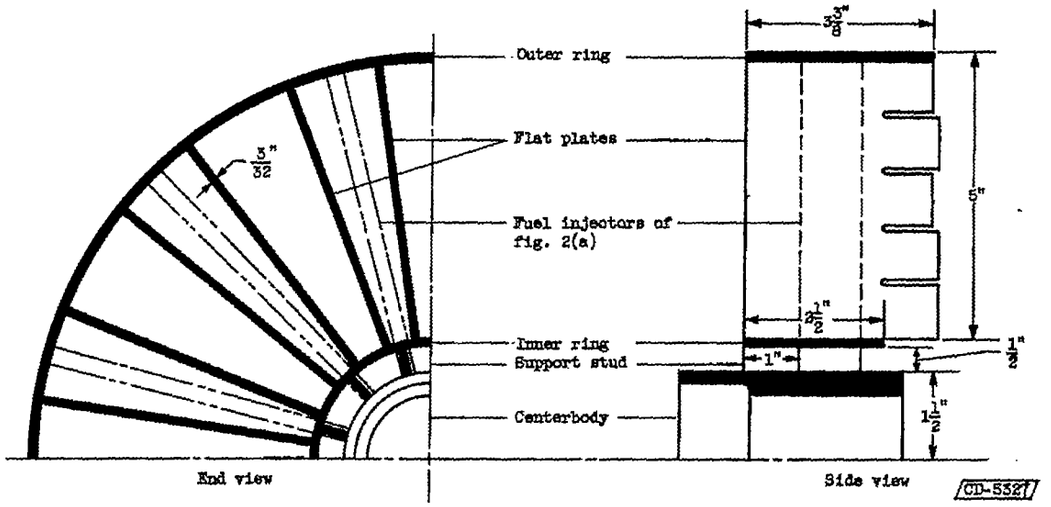

(c) Flameholding shroud of burner 3 before bending tabs.

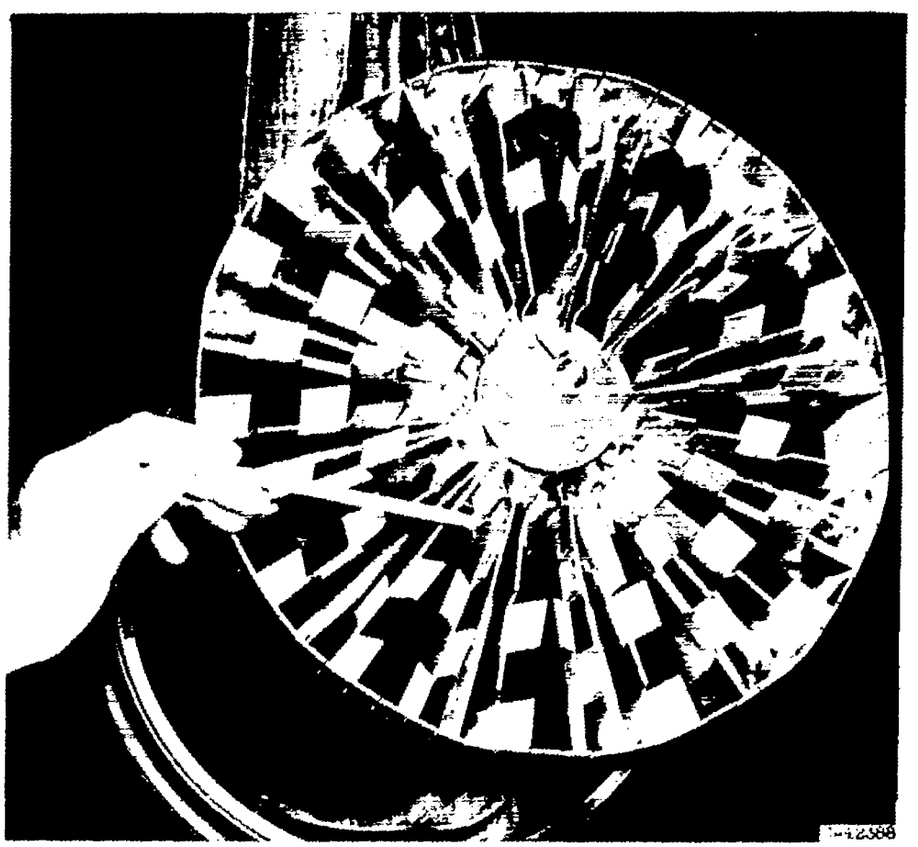

(d) Photograph of burner 3.

Figure 2. - Concluded. Burners investigated.

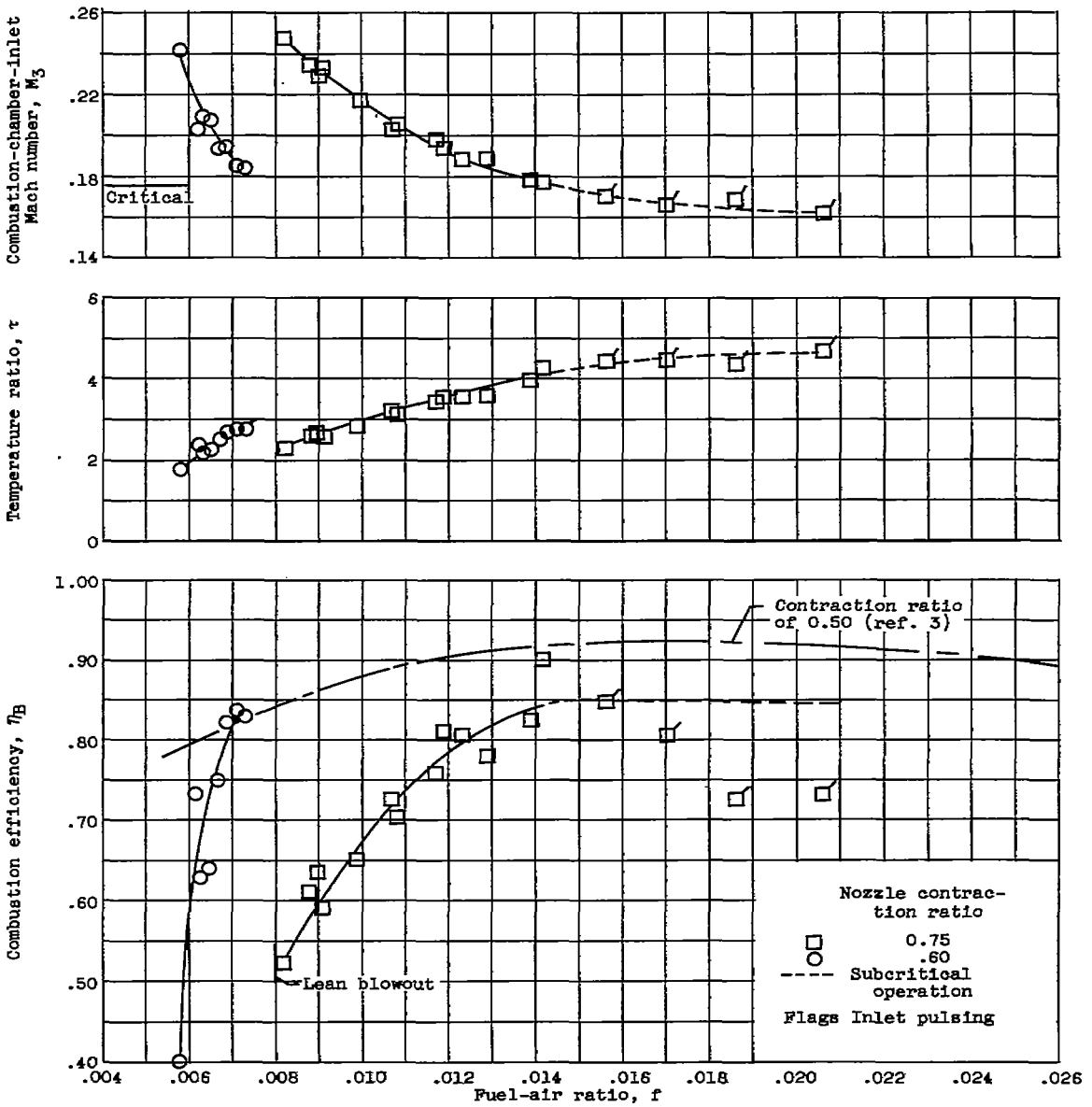

(a) Burner 1.

Figure 3. - General combustor performance with 3-foot tailpipe.

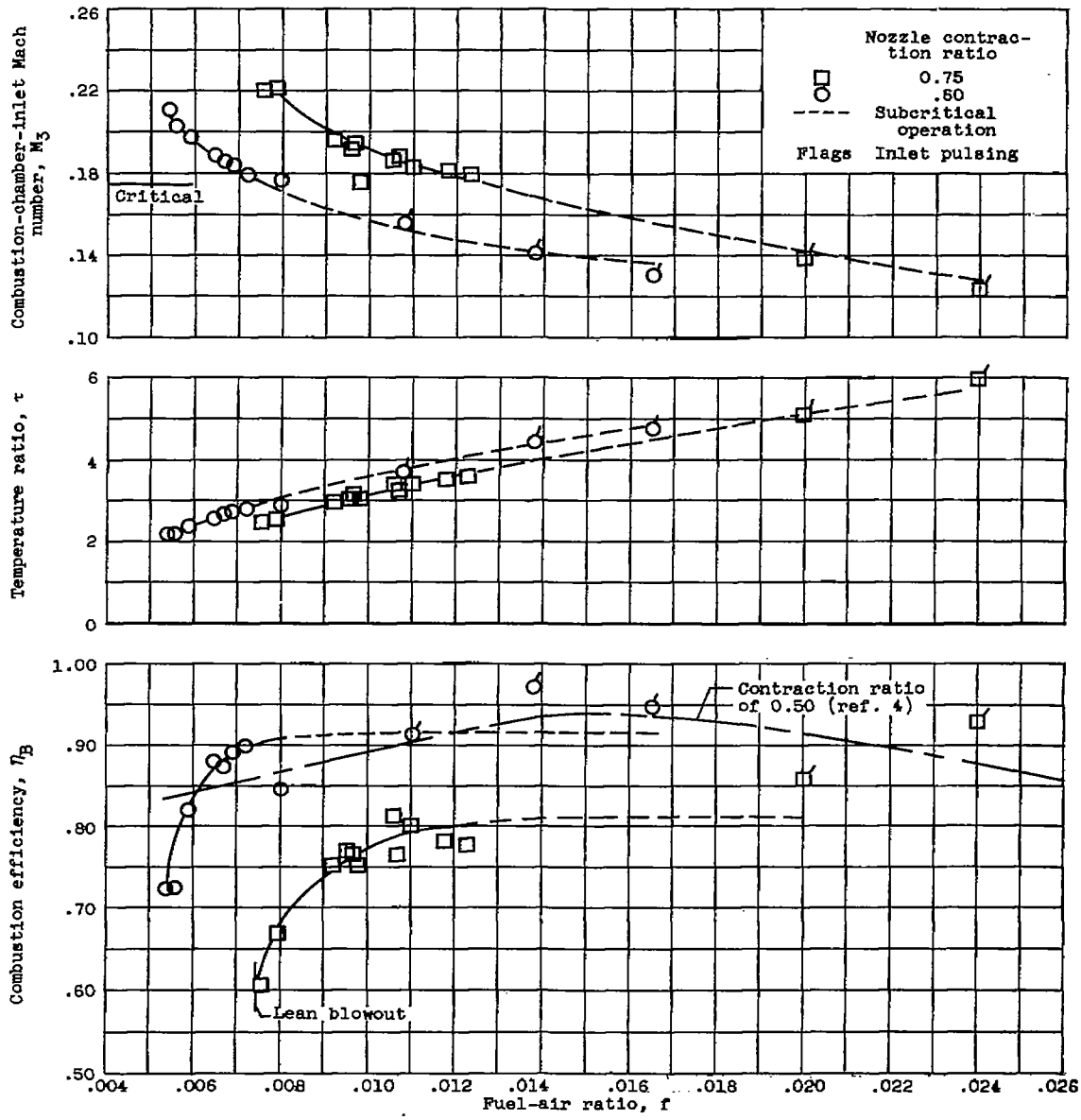

(b) Burner 2.

Figure 3. - Continued. General combustor performance with 3-foot tailpipe.

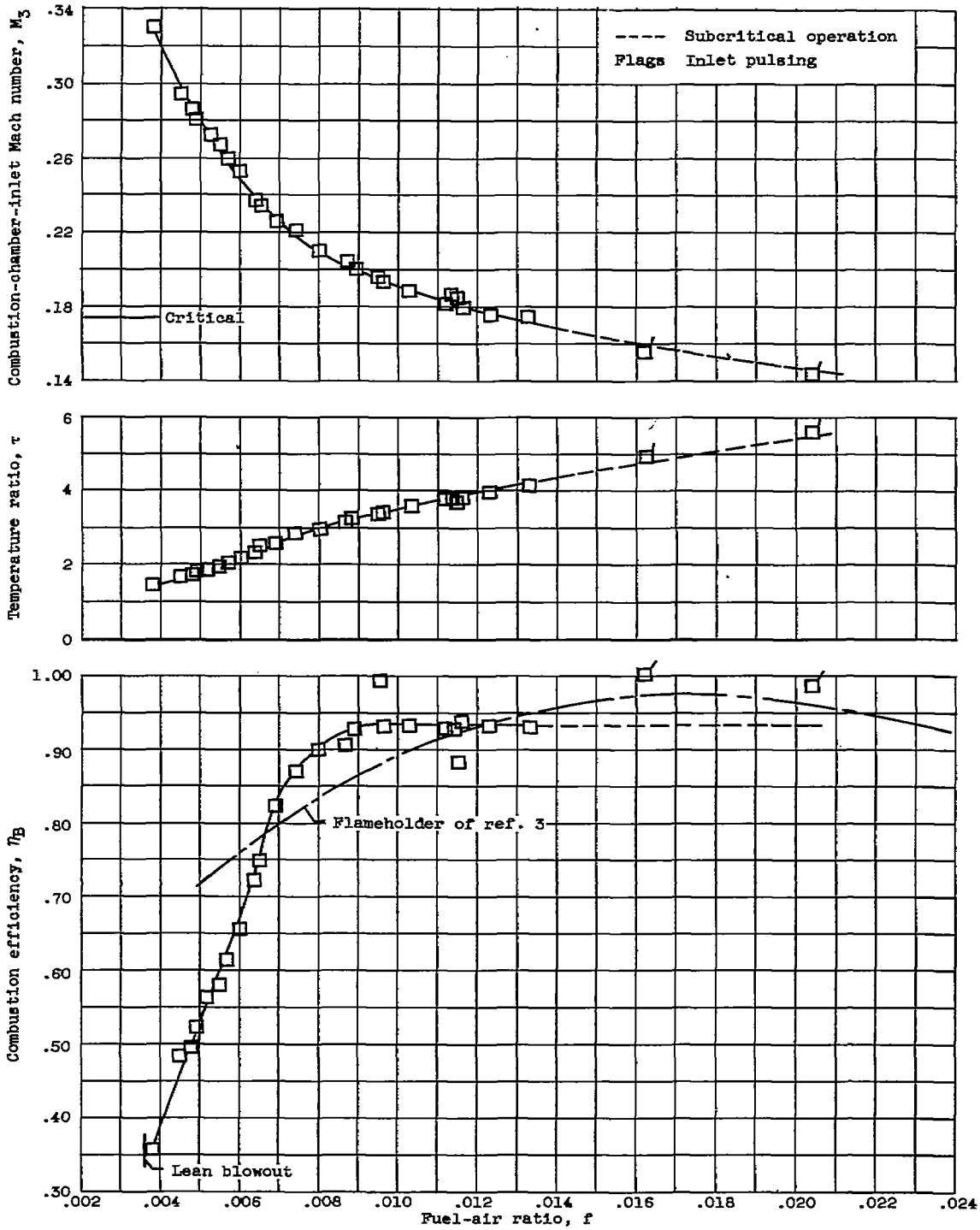

(c) Burner 3. Nozzle contraction ratio, 0.75.

Figure 3. - Concluded. General combustor performance with 3-foot tailpipe.

[redacted]

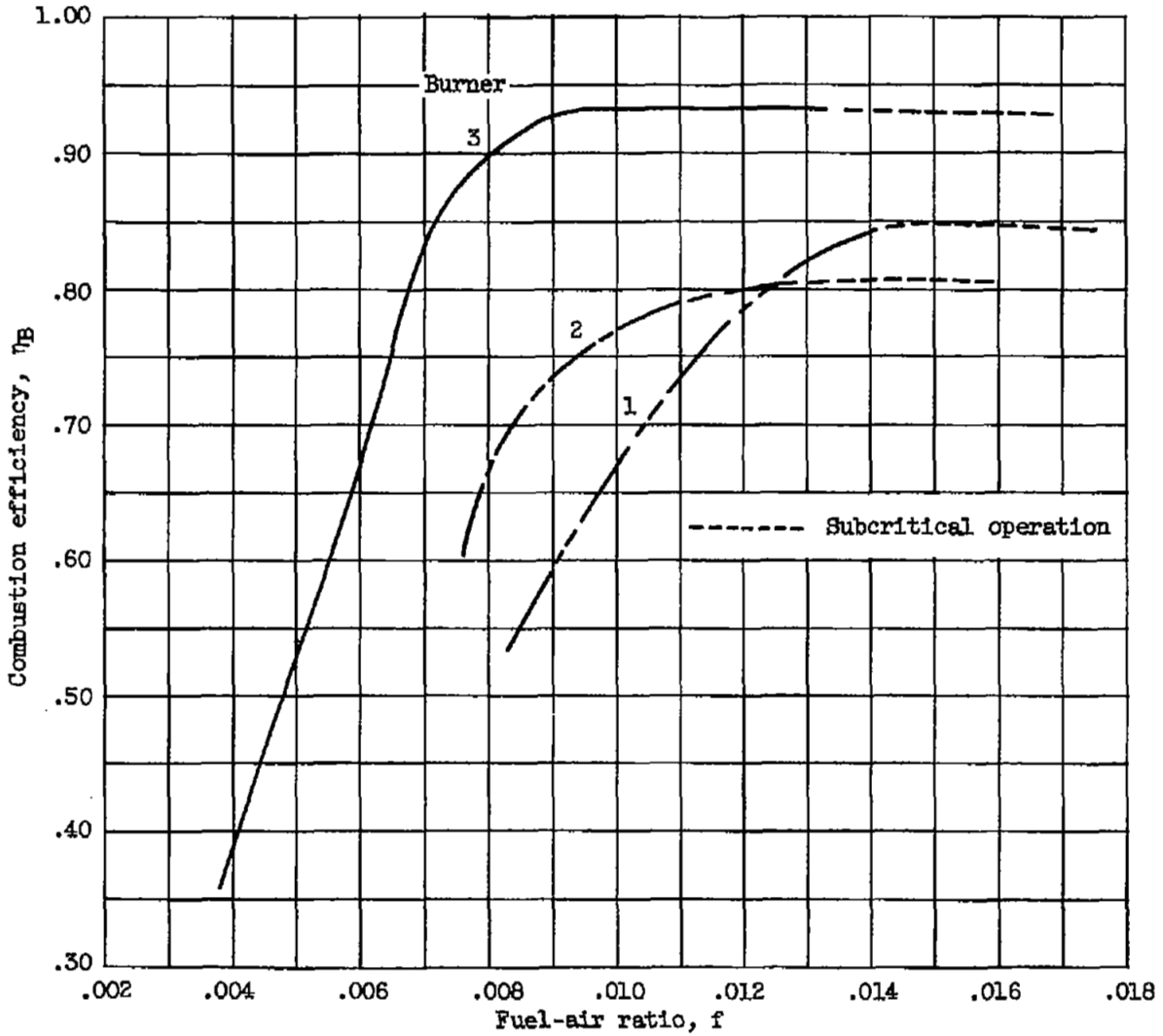

Figure 4. - Summary of efficiencies of burners 1, 2, and 3. Nozzle contraction ratio, 0.75; tailpipe length, 3 feet.

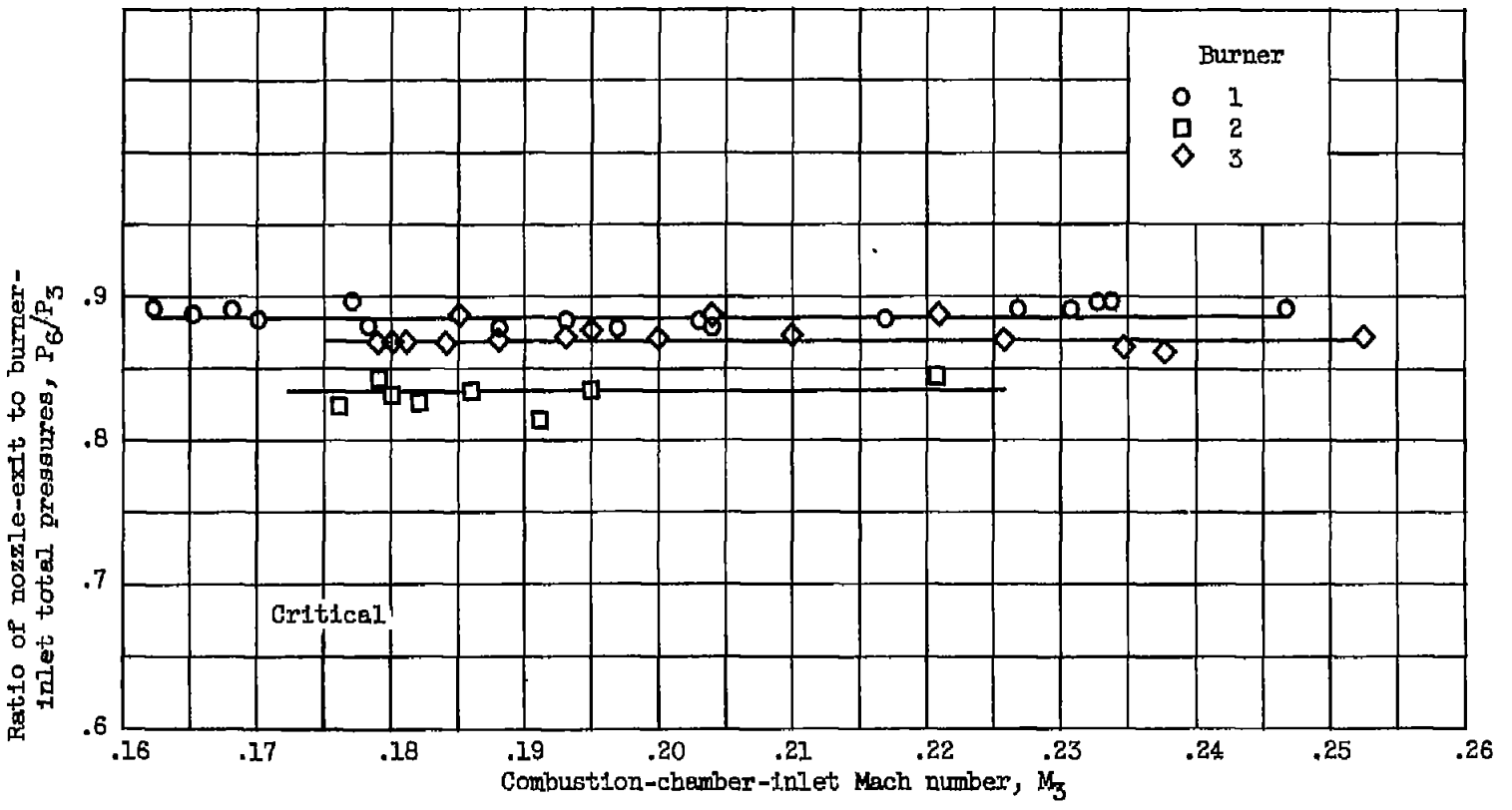

Figure 5. - Combustor total-pressure ratio during burning. Nozzle contraction ratio, 0.75; tail-pipe length, 3 feet.

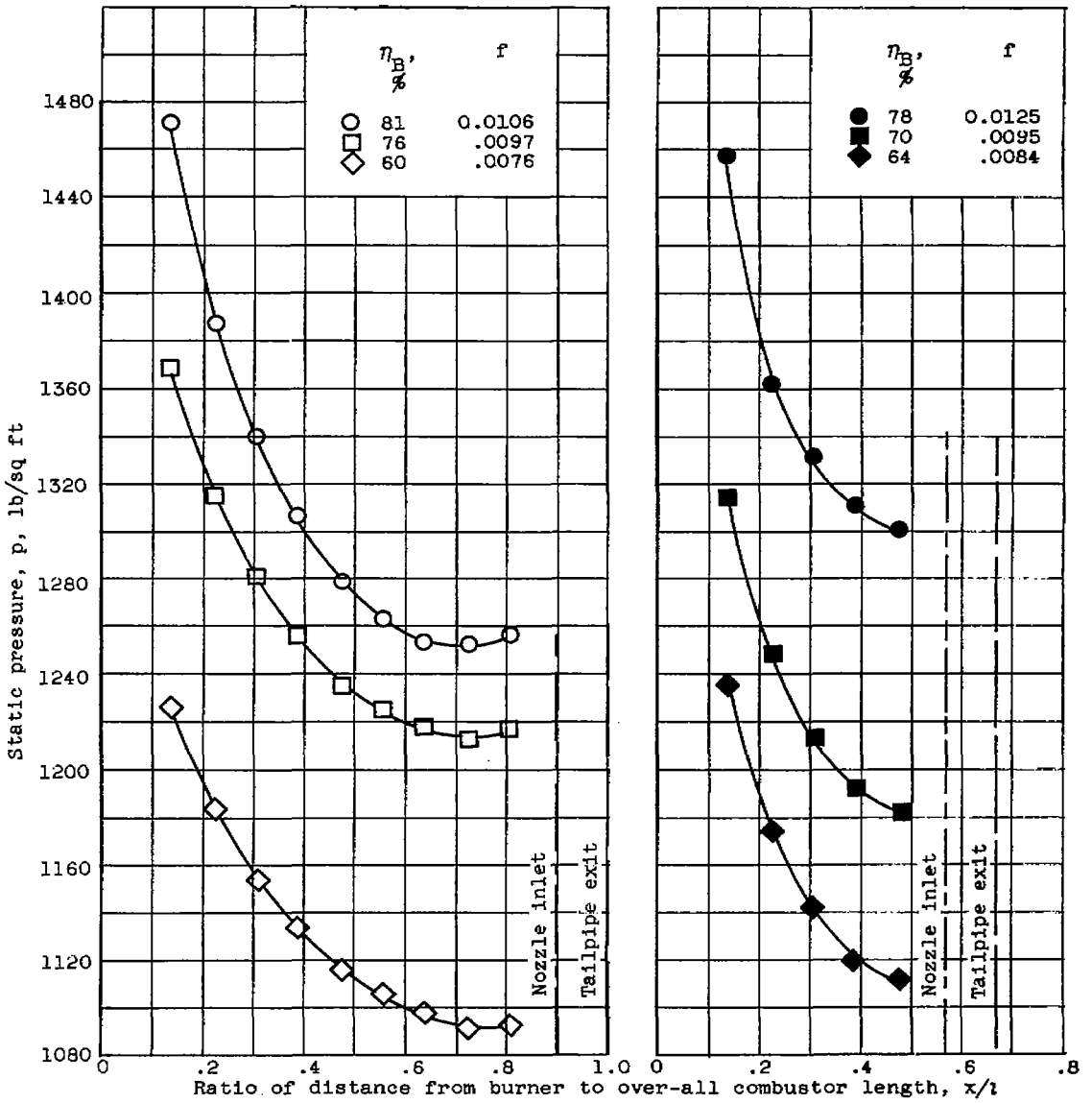

(a) Tailpipe length, 3 feet. (b) Tailpipe length, 2 feet.

Figure 6. - Effect of tailpipe length on combustion with 0.75 nozzle and burner 2.

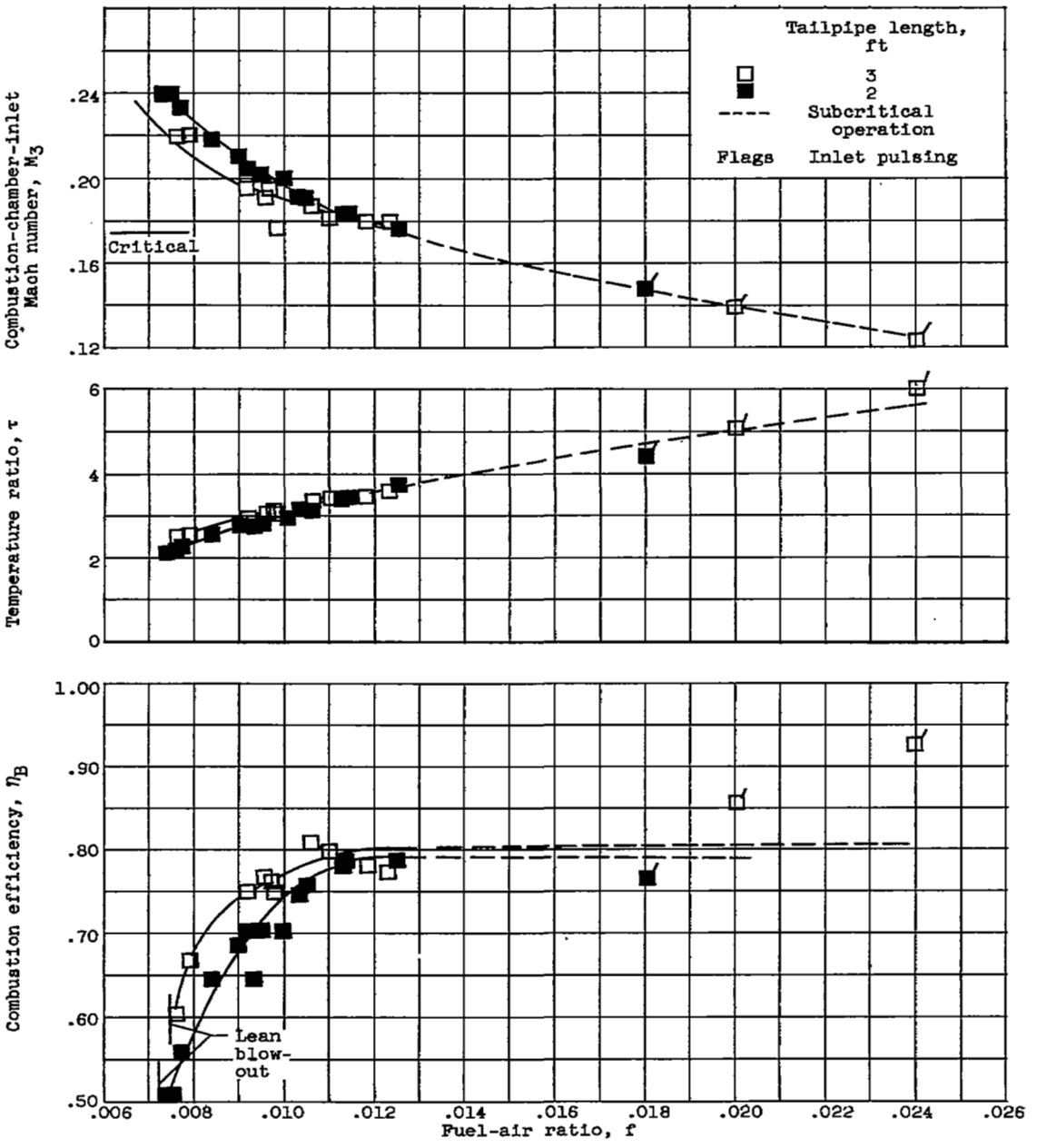

Figure 7. - Effect of tailpipe length on performance of burner 2 with 0.75-contraction-ratio nozzle.

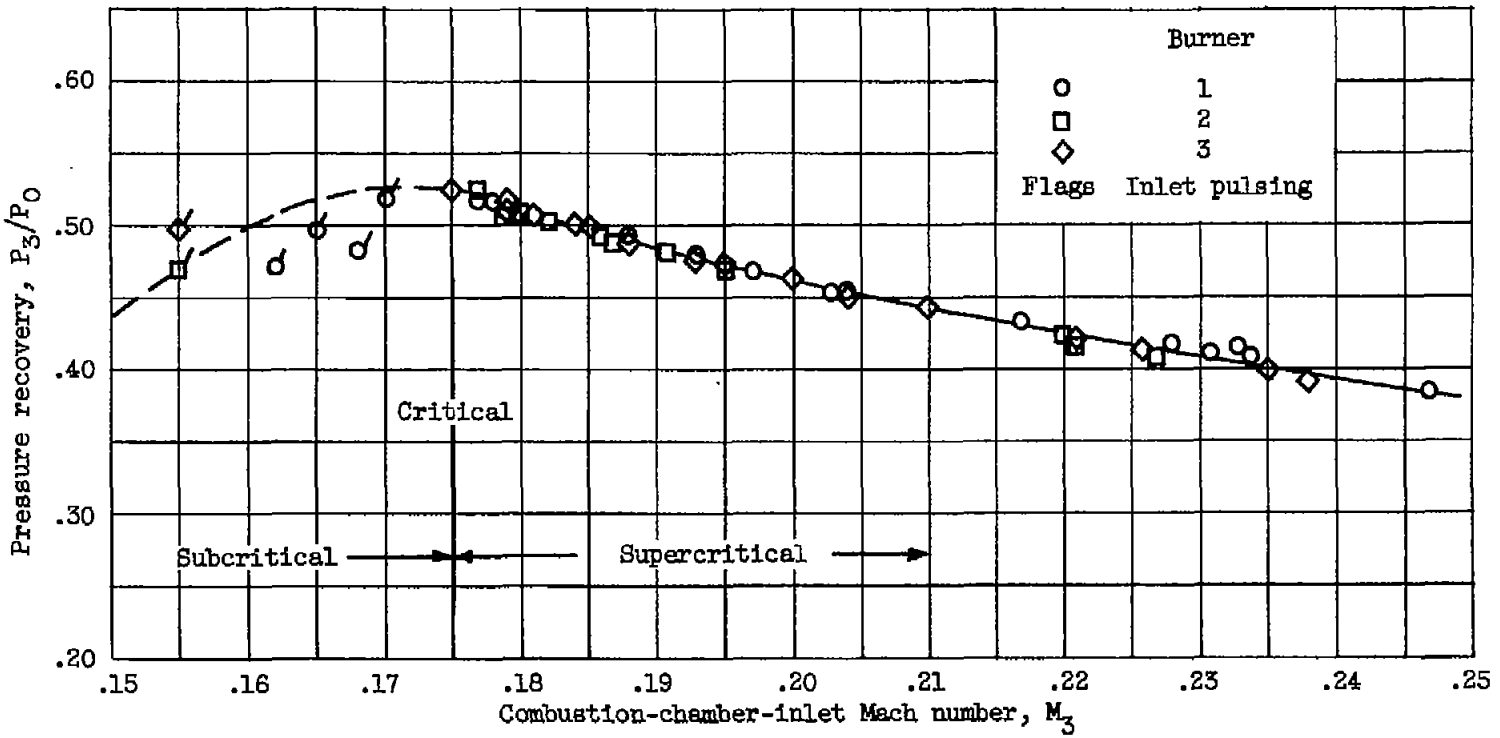

Figure 8. - Diffuser pressure recovery.

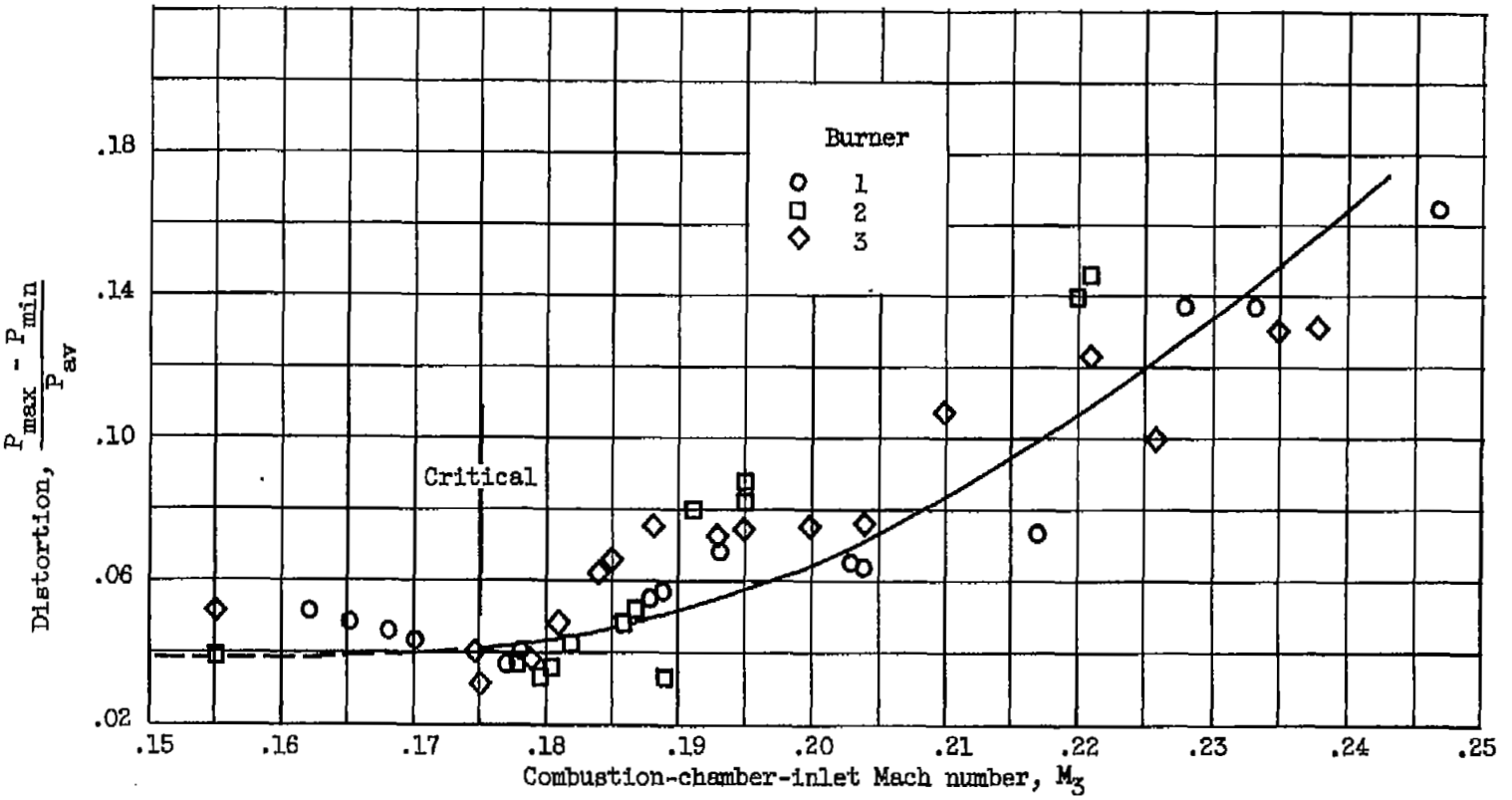

Figure 9. - Burner-inlet distortion level. Nozzle contraction ratio, 0.75; tailpipe length, 3 feet.

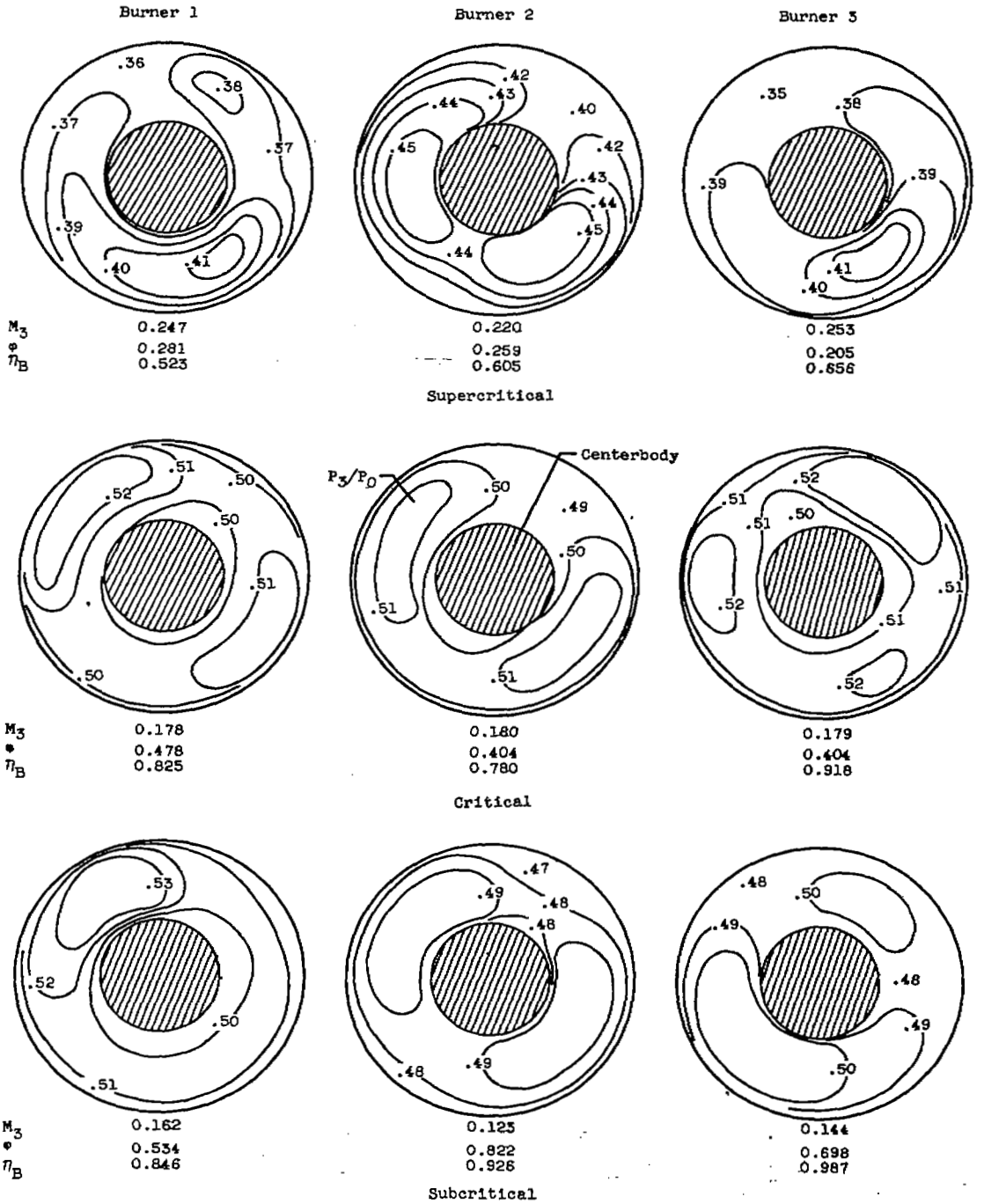

Figure 10. - Typical total-pressure profiles at diffuser exit.

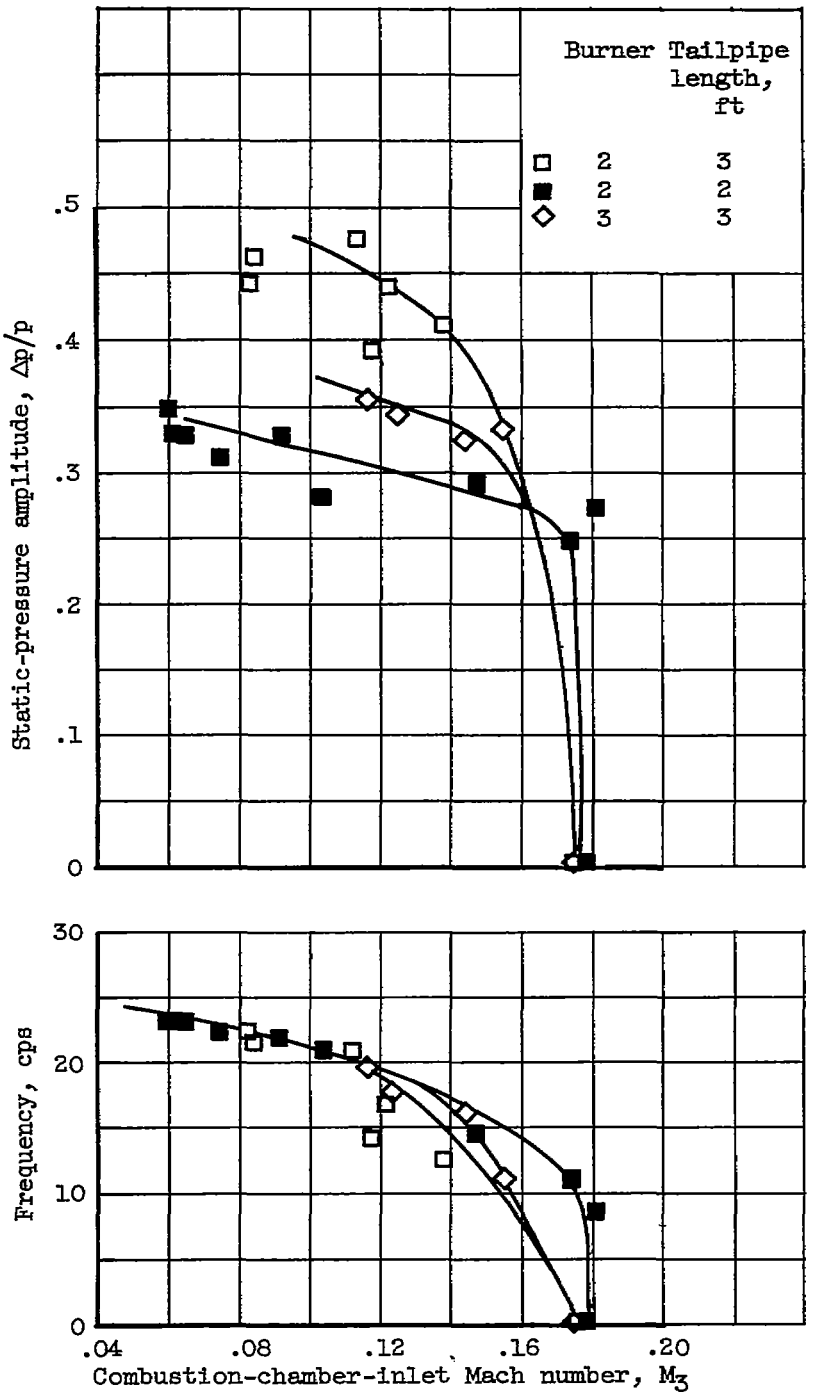

Figure 11. - Static-pressure fluctuations at diffuser exit during burning with 0.75-contraction-ratio nozzle.